

Semiclassical Dynamics of Chaotic Motion: Unexpected Long-Time Accuracy

Steven Tomsovic and Eric J. Heller

Departments of Physics and Chemistry, BG-10, University of Washington, Seattle, Washington 98195

(Received 6 May 1991)

Chaos introduces essential complications into semiclassical mechanics and the conventional wisdom maintains that the semiclassical time-dependent Green's function fails to describe the quantum dynamics once the underlying chaos has had time to develop much finer structure than a quantum cell (\hbar). We develop a method to evaluate the semiclassical approximation and test it for the first time under these circumstances. The comparison of the quantum and semiclassical dynamics of the stadium billiard shows remarkable agreement despite the very intricate underlying classical dynamics.

PACS numbers: 03.65.Sq, 03.40.Kf, 05.45.+b

Semiclassical mechanics has a long, illustrious history of providing both physical insight and approximations to a wide array of quantum-mechanical problems. Being a wave mechanics based solely on input of a classical nature, it focuses all the attention on the properties of a quantum system's classical analog. If the underlying classical dynamics are integrable, the theory is fairly well understood. On the other hand, if the underlying dynamics are chaotic, a number of basic difficulties exist. Indeed, for this situation it was recognized many years ago during the period of the "old quantum theory" that essential complications arose in attempting to approximate stationary quantum solutions [1]. Recently, a great deal of research has been directed toward resolving these problems and yet surprisingly, prior to this work the *fundamental* semiclassical approximation (by which we mean the semiclassical Green's function in the time domain) has never truly been tested for a chaotic system—its validity is quite unknown. One reason for this gap in understanding is a deep rooted, intuitive pessimism about the approximation's applicability since the nonzero size of Planck's constant must be responsible for some kind of smoothing over the intricate complexity that is the essence of chaotic dynamics. This intuition would suggest that phase-space structures on a scale much finer

than \hbar cannot be relevant. A typical argument stresses, for example, that it is easy to find a perturbation which, though barely affecting the quantum system, radically alters each of the classical trajectories—the correspondence principle is failing. A further explanation of this gap lies in the technical difficulty of just evaluating the formal semiclassical expression. In this Letter, we shall outline a method that we have developed for performing the evaluation and demonstrate the astonishingly quantitative agreement existing between the quantum and semiclassical dynamics for a chaotic system, the stadium billiard. This agreement extends well past the time when classical structure far finer than a quantum cell is put into the semiclassical mechanics.

Our starting point is to consider the quantum-mechanical time-dependent Green's function in a coordinate representation. It is denoted

$$G(\mathbf{q}, \mathbf{q}'; t) = \langle \mathbf{q} | e^{-i\hat{H}t/\hbar} | \mathbf{q}' \rangle, \quad (1)$$

where \hat{H} is a quantum Hamiltonian. The propagation of an initial state $\Psi(\mathbf{q}; 0)$ is then given as

$$\Psi(\mathbf{q}; t) = \int_{-\infty}^{\infty} d\mathbf{q}' G(\mathbf{q}, \mathbf{q}'; t) \Psi(\mathbf{q}'; 0). \quad (2)$$

The fundamental approximation is to replace $G(\mathbf{q}, \mathbf{q}'; t)$ with a semiclassical version, $G_{sc}(\mathbf{q}, \mathbf{q}'; t)$ [2],

$$G(\mathbf{q}, \mathbf{q}'; t) \approx G_{sc}(\mathbf{q}, \mathbf{q}'; t) = \left(\frac{1}{2\pi i \hbar} \right)^{d/2} \sum_j \left| \det \left(\frac{\partial^2 S_j(\mathbf{q}, \mathbf{q}'; t)}{\partial \mathbf{q} \partial \mathbf{q}'} \right) \right|^{1/2} \exp \left(\frac{iS_j(\mathbf{q}, \mathbf{q}'; t)}{\hbar} - \frac{i\pi\nu_j}{2} \right). \quad (3)$$

In this expression, the sum over j is for all trajectories connecting \mathbf{q}' to \mathbf{q} in time t , d is the number of degrees of freedom, the prefactor involving the determinant is playing the role of the square root of a classical probability, and the phase is determined by the classical action $S_j(\mathbf{q}, \mathbf{q}'; t)$ and the count of conjugate points (like focal points) ν_j . $S_j(\mathbf{q}, \mathbf{q}'; t)$ is specified by the time integral of the Lagrangian \mathcal{L} ,

$$\begin{aligned} S_j(\mathbf{q}, \mathbf{q}'; t) &= \int_0^t dt' \mathcal{L} \\ &= \int_0^t dt' \{ \mathbf{p}(t') \cdot \dot{\mathbf{q}}(t') - H(\mathbf{p}(t'), \mathbf{q}(t')) \}, \end{aligned} \quad (4)$$

along the j th classical path (H is the classical Hamiltonian).

Equation (3) has been referred to here as the fundamental approximation because it is the starting point of all other forms of semiclassical theory for *chaotic* systems. The most important variants are periodic-orbit theories, as initiated and embodied in the work of Gutzwiller [3]. They extract spectral information from the knowledge of the classical periodic orbits. Attempts to reproduce detailed spectra have proven difficult and have met with only limited success [4]. Justification of these

techniques is still unclear [5] and must ultimately derive from the validity of the dynamical approximation.

Although Eq. (3) formally gives the semiclassical dynamics, as it stands it is prohibitively complicated to calculate—i.e., trajectories of all energies and complexity must be incorporated. In addition, $G_{sc}(\mathbf{q}, \mathbf{q}'; t)$ suffers from a proliferation of singularities in the determinant prefactor due to the coalescence of stationary phase points associated with caustics (a generalization of classical turning points) [6]. Our approach to avoiding these difficulties begins with applying $G_{sc}(\mathbf{q}, \mathbf{q}'; t)$ to the propagation of initially localized wave packets. In this way, the singularities are avoided [7] and only trajectories within some energy window will be relevant, thus eliminating the infinitely complicated orbits. This does not fully solve the technical problem since there is still an uncountable number of quite complicated, contributing orbits. To further simplify the task at hand, we shall concentrate on correlation functions of the type

$$C_{ab}(t) = \langle \Phi_a(0) | \Phi_b(t) \rangle \\ = \int_{-\infty}^{\infty} d\mathbf{q} d\mathbf{q}' \Phi_a^*(\mathbf{q}; 0) G(\mathbf{q}, \mathbf{q}'; t) \Phi_b(\mathbf{q}'; 0), \quad (5)$$

where $\Phi_a(\mathbf{q}; 0)$ and $\Phi_b(\mathbf{q}; 0)$ are wave packets of the form

$$\Phi(\mathbf{q}; 0) = (\pi\sigma^2)^{-d/4} \exp \left[-\frac{(\mathbf{q} - \mathbf{q}_0)^2}{2\sigma^2} + \frac{i\mathbf{p}_0 \cdot (\mathbf{q} - \mathbf{q}_0)}{\hbar} \right]. \quad (6)$$

The centroid, $(\mathbf{q}_0, \mathbf{p}_0)$, determines the region of “phase space” around which the wave packet is localized. Note that the correlation functions entail no loss of generality since all the information contained in $G(\mathbf{q}, \mathbf{q}'; t)$ is also contained in the full set of possible $C_{ab}(t)$.

The first task is to identify all those trajectories that will contribute to $C_{ab}(t)$ within the time interval of interest. The trajectories necessarily begin in the neighborhood of the centroid of $\Phi_b(0)$, $(\mathbf{q}_0, \mathbf{p}_0)_b$, and finish near the centroid of $\Phi_a(0)$, $(\mathbf{q}_0, \mathbf{p}_0)_a$. The procedure for locating trajectories is tantamount to solving the problem of calculating a classical version of $C_{ab}(t)$ where localized classical densities of phase points are used in lieu of wave packets. The details will be published elsewhere [8] and here we just roughly describe the main idea. Illustrated schematically in Fig. 1 are the principle features of chaos upon which we rely. Basically, any initial density of phase points being propagated preserves its volume (Liouville’s theorem), and the phase space has a local hyperbolic structure, meaning that nearby trajectories are either separating or approaching each other exponentially fast. An initially smooth, localized density rapidly evolves and becomes like the filamentary strand pictured. Assuming the accessible phase space is bounded, the filamentary density rapidly folds over upon itself with the number of “folds” proliferating exponentially in time. The intersection of the various branches of the filamentary



FIG. 1. A schematic illustration of the hyperbolic structure of phase space. The initial swarm of trajectories, the black disk, exponentially stretches apart as time evolves from upper left to lower right. The gray disks indicate the initial swarm.

ry density with the neighborhood of $(\mathbf{q}_0, \mathbf{p}_0)_a$ identifies the end points of all the trajectories contributing to $C_{ab}(t)$.

The trajectories are naturally grouped into subsets labeled by the branch in which their end points reside. All the trajectories within a particular subset are exceedingly similar in their properties and it suffices to locate a single member within a branch in order to understand the behavior of all the members of a subset. For a system with two degrees of freedom, it is a simple matter to locate the one reference trajectory per subset referred to as being “heteroclinic” to the classical points $(\mathbf{q}_0, \mathbf{p}_0)_b$ and $(\mathbf{q}_0, \mathbf{p}_0)_a$ [8]. With these heteroclinic orbits, the characterization of a subset follows by linearizing the dynamics in their neighborhoods. The linearization amounts to Taylor expanding the action $S_j(\mathbf{q}, \mathbf{q}'; t)$ in \mathbf{q} and \mathbf{q}' to quadratic order and evaluating the prefactor (which is locally constant); see [9] for a complete summary. In this way, only elementary Gaussian integrals (which are done analytically) are encountered in evaluating Eq. (5) semiclassically. Although, the linearized $S_j(\mathbf{q}, \mathbf{q}'; t)$ is valid only in a small neighborhood around its reference trajectory, the integration with $\Phi_a(\mathbf{q}; 0)$ serves very effectively to cut off this domain. The expression for $C_{ab}(t)$ is reduced to a sum over contributions, one from each subset γ ,

$$C_{ab}(t) \approx \sum_{\gamma} \langle \Phi_a(0) | \Phi_b(t) \rangle_{\gamma}. \quad (7)$$

Technically speaking, this is a sum of contributions over the numerous heteroclinic excursions. The result depends only on the parameters describing each excursion and the local stability of the dynamics.

A good testing ground of the semiclassical dynamics is

provided by the well studied quantized stadium billiard. The classical stadium is proven chaotic (is highly unstable) and there is every reason to believe that the semiclassical dynamics should function in a way typical of many chaotic systems. If a localized wave packet of the form given in Eq. (6) is propagated, it will very rapidly spread to fill the entire stadium. For example, in Fig. 2 are the contours of the real part of a wave packet initially located at the center of the stadium moving toward the right. Scaling the time for the wave packet's horizontal traversal of the stadium to be $t=1$, the propagated wave function is shown for $t=0,1,2,6$. By $t=2$, the time of the shortest unstable periodic orbit, the wave function has already passed the "Ehrenfest time," i.e., it is barely recognizable as having originated from a localized state. Any obvious quantum-classical correspondence has already passed.

To give a quantitative comparison, consider the autocorrelation function, $C_{bb}(t) = \langle \Phi_b(0) | \Phi_b(t) \rangle$, where $\Phi_b(0)$ is pictured in Fig. 2 at $t=0$. The gross behavior of $C_{bb}(t)$ is easily understood. Its magnitude will begin at 1 and drop to nearly 0 as the propagated wave packet begins to move away. It will remain nearly 0 until $t \approx 2$ when parts of the wave packet will have had the time to travel back and forth across the stadium and generate partial recurrences. Soon thereafter the quantum propagated state seems to be everywhere and $C_{bb}(t)$ will settle into some fluctuating pattern. This is borne out in

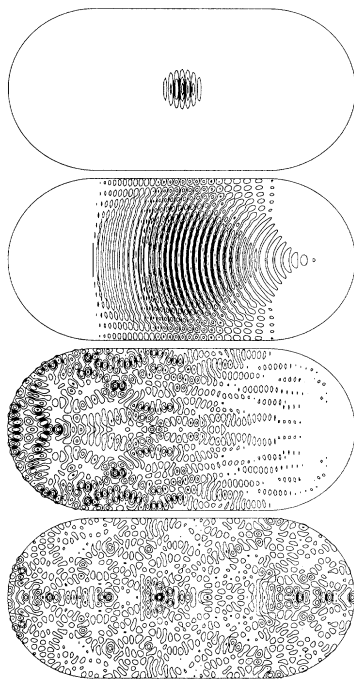


FIG. 2. Evolution of a localized wave packet in the stadium billiard. The initial Gaussian pictured in the first frame is chosen so that 30 wavelengths stretch across the horizontal axis.

Fig. 3(a) by the dashed (exact quantum) curve. The surprise is that every detail of the fluctuating quantum behavior is captured by the semiclassical prediction which is superposed on the same figure as a solid curve. In performing the heteroclinic (homoclinic for autocorrelation functions) summation to obtain the semiclassical prediction, about a dozen orbits were contributing at any given time near $t \approx 2$. By $t \approx 4$, several hundred were contributing, and by $t \approx 5$ or 6, more than 30000 heteroclinic terms were needed in the summation. To picture the dynamical complexity, consider the bottom right image of Fig. 1 which shows 7 branches slicing through the gray disk. To attain $t \approx 5$ or 6, one would have to draw more than 30000 branches fitting in the gray disk. Other than for the beginning of the first recurrence, no individual orbit comes anywhere close to generating the magnitudes of the recurrences seen; all of the terms are necessary. In Fig. 3(b), just the real part of $C_{bb}(t)$ is shown on an expanded scale to display better the quality of agreement. We have checked other cases, including examples with far fewer nodes, i.e., lower energies (and cross correlations, $a \neq b$), and found similar agreement.

Because our method approximates $G_{sc}(\mathbf{q}, \mathbf{q}'; t)$, the already quantitative results could only improve if a better evaluation of the semiclassical dynamics were available. Thus, the intricate dynamics of chaotic motion do not have the strong adverse effect on the fundamental semiclassical approximation that had been believed [10]. Nearly all the thousands of branches of trajectories are *individually* generating accurate contributions to $C_{ab}(t)$;

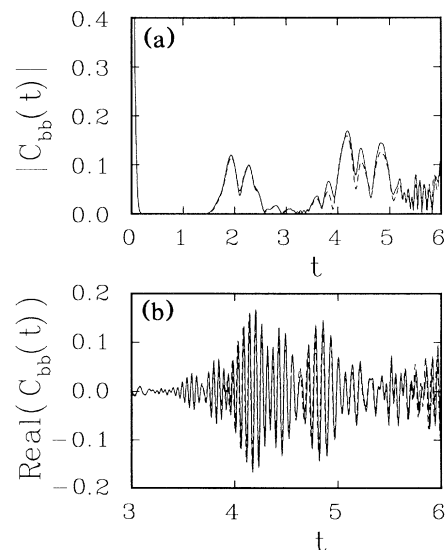


FIG. 3. The comparison of an exact quantum and a semiclassical calculation of an autocorrelation function. The quantum curves are dashed and the semiclassical are solid. (a) The absolute magnitude of $C_{bb}(t)$. (b) A blowup of the real part of $C_{bb}(t)$.

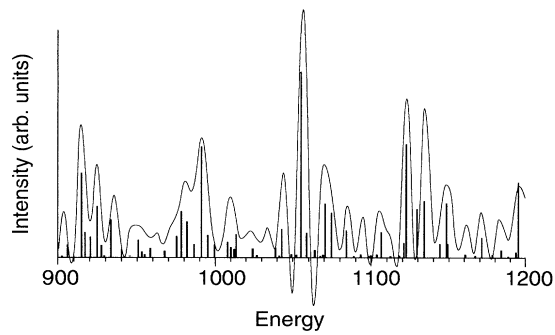


FIG. 4. The time-energy Fourier transform of $C_{bb}(t)$ and spectrum of ϕ_b . The transform is cut off in time abruptly at $t=8$ beyond which the number of heteroclinic orbits required to evaluate Eq. (7) becomes impractical. For display only the center one-third region of the ϕ_b spectrum is shown.

nearby branches do not compromise the accuracy of a given branch.

The overlap intensity of ϕ_b with the eigenstates may be obtained by Fourier transforming the dynamics. Figure 4 shows the comparison of the transformed semiclassics with the exact quantum intensity spectrum. The maximum peak occurs near the 1200th eigenvalue. Remarkably, the semiclassical theory is reproducing the quantum fine structure to the scale of 2 to 3 mean spacings. The limit of resolution results from the present practical limit of performing the classical dynamics and not by any failure of the semiclassics. The ability to resolve structure on the scale of an average spacing or less has been a major goal since efforts began on understanding the semiclassical dynamics of chaos.

As quantitative as the results are, clearly there are quantum effects not contained in $G_{sc}(\mathbf{q}, \mathbf{q}'; t)$. As an example, consider the branches for which our technique of evaluating Eq. (7) must break down, i.e., those folded within the overlap region. In the stadium, a fold develops when one of the local trajectories strikes the joint between the semicircular end cap and the straight edge. These folds generate sources of diffraction and that is certainly left out of Eq. (3). Their contributions to the

quantum mechanics must show up, but it is plausible that not all $C_{ab}(t)$ are equally affected, with most being well behaved.

There are several natural continuations of this work that we are pursuing. Examples include (i) understanding better the domain of time and \hbar in which semiclassical arguments are valid, (ii) searching for ways of summarizing the classical information in order to simplify evaluating the heteroclinic summation, (iii) investigating the nature of "chaotic" eigenfunctions incorporating the new-found access to long-time dynamics, (iv) reexamining Gutzwiller periodic-orbit theory for possible corrections and new insight, and (v) further development of the semiclassical techniques for application to physical systems.

We acknowledge fruitful discussions with P. W. O'Connor and R. Legere. This research was supported by the National Science Foundation under Grant No. CHE-9014555.

- [1] See for example, A. Einstein, Ver. Deut. Phys. Ges. **19**, 82 (1917), translated into English by Charles Jaffe, Joint Institute for Laboratory Astrophysics Report No. 116 (unpublished).
- [2] M. C. Gutzwiller, J. Math. Phys. **8**, 1979 (1967).
- [3] M. C. Gutzwiller, J. Math. Phys. **12**, 343 (1971), and references therein.
- [4] M. C. Gutzwiller, Physica (Amsterdam) **5D**, 183 (1982); M. Sieber and F. Steiner, Physica (Amsterdam) **44D**, 248 (1990); some very recent advances hold much promise, for example, see G. Tanner, P. Scherer, E. B. Bogomolny, B. Eckhardt, and D. Wintgen, report (to be published).
- [5] A. Voros, J. Phys. A **21**, 685 (1988).
- [6] M. V. Berry, N. L. Balazs, M. Tabor, and A. Voros, Ann. Phys. (N.Y.) **122**, 26 (1979).
- [7] Eric J. Heller, J. Chem. Phys. **67**, 3339 (1977).
- [8] Steven Tomsovic and Eric J. Heller (to be published).
- [9] E. J. Heller, in *Chaos and Quantum Physics*, edited by M. J. Giannoni, A. Voros, and J. Zinn-Justin (Elsevier Science, Amsterdam, 1990).
- [10] Similar conclusions were also reached in work on the quantum baker's map by P. W. O'Connor, S. Tomsovic, and E. J. Heller (to be published).